An Analytic Method of Segmented PWM Duty Cycle for Switched Reluctance Motor

Chaozhi Huang, *Member, CES*, Yuliang Wu, Hongwei Yuan, Wensheng Cao, and Yongmin Geng

***Abstract*—In view of the large current peak and torque ripple in the actual current chopping control of switched reluctance motor, a segmented PWM duty cycle analysis method of switched reluctance motor based on current chopping control is proposed in this paper. The method realizes the control of the winding current by adjusting the average voltage of the two ends of the winding in one cycle through the PWM duty cycle. At the same time, according to the inductance linear model, the conduction phase is divided into a small inductance region and an inductance rising region, and the analytical formulas of PWM duty cycle in the two regions are deduced respectively. Finally, through matlab/simulink simulation and motor platform experiment, the current chopping control is compared with the segmented PWM duty cycle analysis method in this paper. Simulation and experimental results show that the segmented PWM duty cycle analysis method can effectively reduce the current peak and torque ripple, and has high practical application value.**

***Index Terms*—Switched Reluctance Motor, Current Chopping Control, PWM Duty Cycle, Current Peak, Torque Ripple.**

I. INTRODUCTION

SWITCHED reluctance motor(SRM) has a simple structure, a wide speed regulation range and can operate in a wide speed range. It has a broad application prospect in the new energy vehicle industry, and has attracted extensive attention from scholars and business circles all over the world [1]. Switched reluctance motors often use current chopping control(CCC) at low speed or start-up, but due to the current sampling frequency, power tube switching frequency and other factors, the current will exceed the hysteresis loop range in actual control, which will significantly increase the motor winding loss and torque ripple [2].

In order to solve the above problems, many methods have been proposed at home and abroad. In terms of current control, Q. N. Li proposed a deadbeat current control strategy, which makes the current control command easier and plays an obvious role in suppressing torque ripple [3]. X. Zhang also adopted the deadbeat current control method to improve the phase current control accuracy, which also has a good effect in suppressing current ripple [4]. In order to improve the current tracking performance, S. Q. Shen predicted the average voltage required for the actual current of the next cycle according to the voltage and current of the previous cycle [5]. S. K. Sahoo can track the given current at the fixed rotor position by iterative learning control of the voltage at the fixed rotor position [6], [7]. To further speed up the tracking, scholars also proposed a reinforcement learning method [8]. M. Y. Ma adopted fuzzy control strategy to automatically adjust the harmonic current coefficient of each section [9]. F. Peng proposed an adaptive controller, which has approximately the same dynamic response and accuracy as the hysteresis controller [10]. For the suppression of torque ripple, some scholars have proposed an optimized pulse width modulation (PWM) control. Accurately predict the voltage ratio and duty cycle according to the information of motor operating parameters [11], [12]. Y. Cheng and C. Zhao combined both direct instantaneous torque control (DITC) and PWM control with segmented control. The results show that the proposed method can reduce the inherent torque ripple [13], [14]. Scholars also proposed a new active vibration cancellation (AVC) control for variable-speed SR motor drives under digital PWM control to suppress the vibration that occurs on the stator body during commutation [15]. Z. Y. Yu proposed a simplified pulse width modulation strategy to achieve switching action minimization and common mode voltage (CMV) reduction [16].

In this paper, a segmented PWM duty cycle analysis method based on current chopping control is proposed for the situation of large overshoot current and large torque ripple. Combined with the current characteristics of small inductance region and inductance rising region, the average voltage required for the two regions in real time is deduced respectively. At the same time of current chopping control, PWM duty cycle is used to adjust the average voltage at both ends of the conducting phase winding to realize the control of winding current. Finally, the effectiveness of the proposed method is verified by simulation experiments and motor experiments, which provides a new idea to improve the current tracking performance and reduce torque pulsation in switched reluctance motors.

II. CURRENT CHOPPER CONTROL

The main factors affecting the operation performance of switched reluctance motor are the phase current waveform, the

Manuscript received July 22, 2022; revised August 11, 2022; accepted August 24, 2022. Date of publication June 25, 2023; Date of current version January 11, 2023.

This work was supported by National Natural Science Foundation of China under Grant 52167005, Science and Technology Research Project of Jiangxi Provincial Department of Education under Grant GJJ200826.

(Corresponding Author: Yuliang Wu)

Chaozhi Huang, Yuliang Wu, Hongwei Yuan, Wensheng Cao, and Yongmin Geng are with the School of Electrical and Automation, Jiangxi University of Science and Technology, Ganzhou, 341000, China (e-mail: huangchaozhi@163.com, wuyuliang1016@163.com, 2550747126@qq.com, 554859697@qq.com, 569474503@qq.com,)

Digital Object Identifier 10.30941/CESTEMS.2023.00008

current peak value and the position of peak value. Since the nonlinear characteristics of SRM are mainly related to $L(\theta, i)$ and $i(\theta)$ and are difficult to analyze. For practical reasons, it can be analyzed from a linear model. Assuming that the motor phase current is independent of the inductance, and ignoring the saturation effect and the magnetic field edge diffusion effect, the curve of the phase winding inductance periodically changing with the rotor position angle θ is shown in Fig. 1.

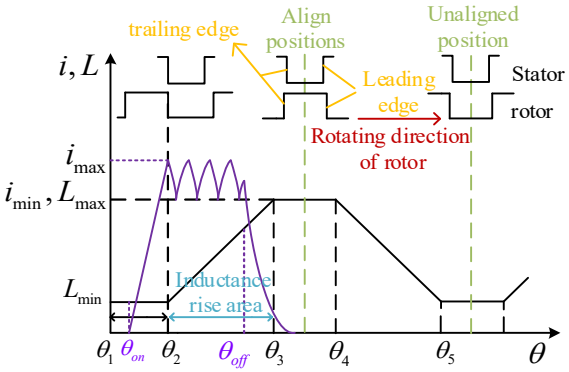

Fig. 1. Relationship between phase winding inductance and rotor position.

θ_1 corresponds to the alignment position between the stator salient pole and the rotor groove centerline, and the inductance is the smallest at this time. θ_2 corresponds to the alignment position between the leading edge of the rotor pole and the trailing edge of the stator pole, θ_3 corresponds to the position where the leading edge of the rotor pole and the leading edge of the stator pole are aligned, and the region θ_2-θ_3 is the inductance rising area, and the inductance reaches its maximum value at θ_3. The phase inductance analytical formula corresponding to the linear model can be expressed as:

$$L(\theta)=\begin{cases} L_{\min} & \theta_1 \le \theta \le \theta_2 \\ K(\theta-\theta_2)+L_{\min} & \theta_2 \le \theta \le \theta_3 \\ L_{\max} & \theta_3 \le \theta \le \theta_4 \\ L_{\max}-K(\theta-\theta_4) & \theta_4 \le \theta \le \theta_5 \end{cases} \tag{1}$$

In the formula, θ is the electrical angle of the rotor, $L_{\max}$ is the maximum inductance, $L_{\min}$ is the minimum inductance, and K is the change slope of the inductance. The value of K can be obtained from Fig. 1:

$$K=\frac{L_{\max}-L_{\min}}{\theta_3-\theta_2} \tag{2}$$

Ignoring the flux saturation, the electromagnetic torque equation of SRM in the ideal linear model is:

$$T_{total}(i,\theta)=\sum_{k=1}^{m}\frac{1}{2}i^2\frac{dL(i,\theta)}{d\theta} \tag{3}$$

In the formula, i is winding phase current, $L(i, \theta)$ is the winding phase inductance, θ is the rotor position angle, m is the number of phases of the motor.

It can be seen from (3) that torque is related to phase current and rotor position angle, so controlling phase current at different position angles can change the instantaneous torque of SRM. When SRM is operating below base speed, current chopping control strategy is usually adopted to avoid excessive phase current.

The current chopping control usually has a fixed turn-on angle and turn-off angle, and the phase current is controlled to maintain the desired value by the given upper current amplitude $i_{\max}$ and lower amplitude $i_{\min}$. If the current exceeds $i_{\max}$, the power tube is turned off, forcing the current down. If the current decreases to $i_{\min}$, the power tube is turned on, and the current starts to increase again. Fig. 2 shows the current waveform of current chopping control.

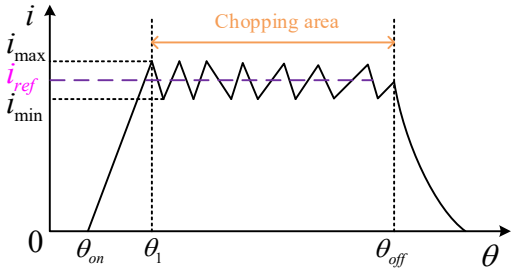

Fig. 2. Phase current waveform under current chopper control.

In the actual current chopping control, the control signal will be delayed due to the influence of current sampling frequency, controller calculation performance and power tube switching frequency. When the current changes too fast, the winding current of one sampling period will easily exceed the upper and lower limits of the hysteresis loop, which will generate large overshoot current and current ripple. Excessive current ripple can damage the semiconductor components in the driver, greatly reducing its service life, and lead to large torque ripple, which will affect the performance of the electric drive system. Fig. 3 shows the current chopping control block diagram.

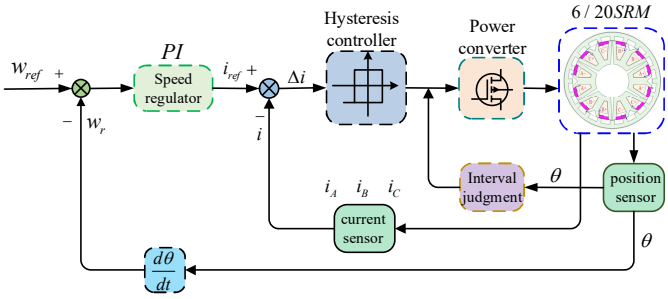

Fig. 3. Current chopping control block diagram.

III. Analytic Method Of Segmented PWM Duty Cycle

The change of winding current is influenced by the voltage at both ends of the winding. Therefore, the winding current can be controlled by adjusting the average voltage at both ends of the conducting phase winding, that is, PWM duty cycle, thereby reducing the overshoot current and torque ripple.

A. Analytical Formula of PWM Duty Cycle In The Region $\theta_1<\theta<\theta_2$

In this region, the SRM inductance remains basically constant and the inductance is the minimum value. In order to obtain a better output torque and reduce the winding loss in the actual control, the winding current is required to reach the given current at θ_2. The winding voltage balance equation of the k-th phase of the SRM is:

$$U_k=i_kR_k+\frac{d\varphi}{dt} \tag{4}$$

In the formula, U_k is the voltage across the k-th phase

winding, i_k is the k-th phase winding current, R_k is the k-th phase winding resistance, φ is the phase winding flux linkage. The voltage drop across the winding resistance is so small that it can be ignored in qualitative analysis.

$$U_k = \frac{d\varphi}{dt} = L\frac{di_k}{dt} + i_k\frac{dL}{dt} \tag{5}$$

The inductance in this region remains constant, and its inductance rate of change is zero. The inductance value in this region is recorded as $L_{\min}$.

$$U_k = L\frac{di_k}{dt} = L_{\min} w\frac{di_k}{d\theta} \tag{6}$$

In the formula, w is the angular velocity of the motor. The current change rate in this region can be obtained from (6).

$$\frac{di_k}{d\theta} = \frac{U_k}{L_{\min} w} \tag{7}$$

$$i_k = \int_{\theta_1}^{\theta} \frac{U_k}{L_{\min} w} d\theta \tag{8}$$

Assume an equivalent winding voltage, denoted as U_{k1}, makes the winding current monotonically increase in the region θ_1-θ_2. And the given current is reached at θ_2, that is, $i_k(\theta_2)=i_{ref}$, which improves the current tracking ability.

$$i_k(\theta_2) = \frac{U_{k1}}{L_{\min} w}(\theta_2 - \theta_1) \tag{9}$$

The equivalent winding voltage expression in this region can be obtained from 9.

$$U_{k1} = \frac{i_{ref} L_{\min} w}{(\theta_2 - \theta_1)} \tag{10}$$

In the formula, $w = 2\pi n / 60$, n is the motor speed. Assuming that the DC power supply voltage at both ends of the SRM winding is U_S, the PWM duty cycle in the region θ1-θ2 can be obtained from (10) as U_{k1}/U_S, denoted as σ_1.

$$\sigma_1 = \frac{i_{ref} L_{\min} \pi n}{30(\theta_2 - \theta_1) U_S} \tag{11}$$

B. Analytical Formula of PWM duty Cycle in The Region $\theta_2<\theta<\theta_3$

This region is single-phase conduction. In order to reduce the torque ripple, the winding current in this region can be approximated as i_{ref} and remains unchanged, then there is $di_k/d_t=0$.

$$U_k = \frac{d\varphi}{dt} = i_k\frac{dL}{dt} = i_{ref} w\frac{dL}{d\theta} \tag{12}$$

In the formula, $\frac{dL}{d\theta} = \frac{L_{\max} - L_{\min}}{\theta_3 - \theta_2}$, In this region, it is assumed that the equivalent voltage of the winding is U_{k2}. According to (12), the PWM duty cycle in the region θ_2-θ_3 is U_{k2}/U_S, denoted as σ_2.

$$\sigma_2 = \frac{i_{ref}(L_{\max} - L_{\min})\pi n}{30(\theta_3 - \theta_2) U_S} \tag{13}$$

From (11) and (13), the analytical expressions of PWM duty cycle in two regions can be obtained. PWM_1 and PWM_2 are the driving signals of power tubes under the control of current chopper, and PWM_1' and PWM_2' are the driving signals of power tubes under the control of PWM duty cycle analytical method in this paper. In the region of $\theta_1< \theta <\theta_2$, the upper and lower power tubes are closed, the phase current starts to rise from zero to the given current at θ_2. In the region of $\theta_2< \theta <\theta_3$, the three switching states are selected according to the current error between the actual phase current and the reference current. When the excitation state is "S=1", the circuit operates in the positive voltage excitation state, and the phase current rises rapidly. When the zero voltage freewheeling state is "S=0", the circuit operates in the zero voltage freewheeling state, and the phase current decreases slowly. When the demagnetization state is "S=-1", the circuit operates in the negative voltage demagnetization state, and the phase current decreases rapidly.

After the improvement, the average voltage in the three states is $U_k = (\sigma_1, \sigma_2)U_S < U_S$, so the current rising and falling rates become slower and smaller in the sampling period T_S, and the current ripple and torque ripple can be further improved compared with the current chopper control. Figure 4 shows the three working states of the drive circuit and the drive signal of the power tube.

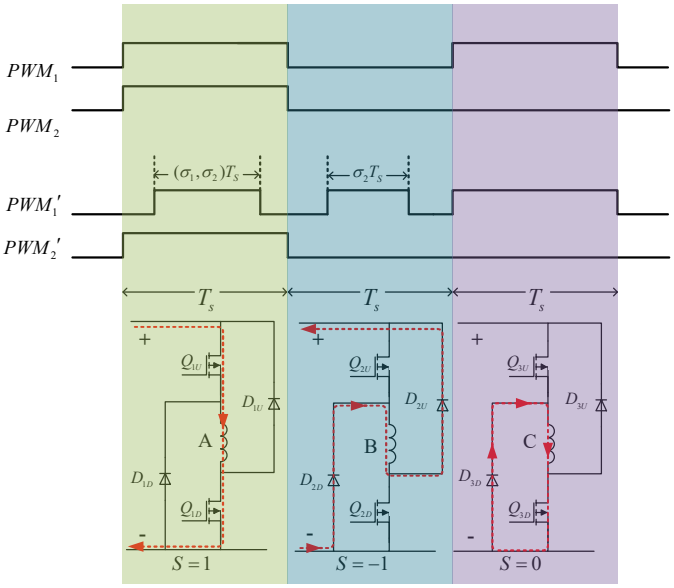

Fig. 4. The three working states of the drive circuit and the drive signal of the power tube.

In this paper, the control strategy uses external speed loop and internal current loop. The region judgment module judges the region of the rotor based on the real-time rotor position angle provided by the position sensor. The current sensor samples the real-time phase current of the motor. The PWM duty cycle analysis module calculates the PWM duty cycle σ_1 and σ_2 according to the region of the rotor position and (11, 13), and then applies the obtained duty cycle to the PWM signal generator to generate the corresponding PWM drive signal to control the power tube. Figure 5 is a control block diagram of the segmental PWM duty cycle analysis method based on current chopping control.

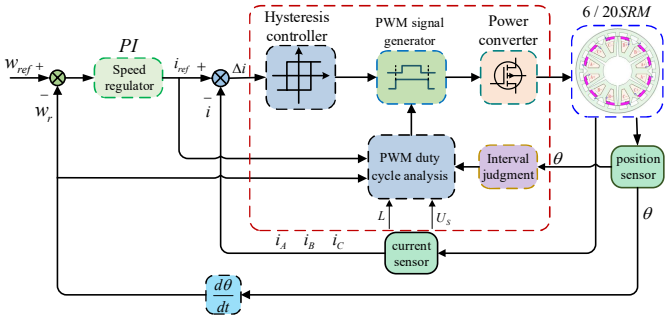

Fig. 5. Control block diagram of segmental PWM duty cycle analysis method based on current chopping control.

IV. Simulation Analysis

In order to verify the effectiveness of the segmented PWM duty cycle analysis method of Switched Reluctance Motor Based on current chopping control proposed in this paper, a control system model of three-phase 6/20 switched reluctance motor prototype is built on matlab/simulink.

In the simulation experiments, the turn-on angle of 0.5º and the turn-off angle of 7.5º are fixed. Since current chopping is mostly used in low speeds, the given speeds of the simulation experiments in this paper are 500r/min and 750r/min, respectively, and the loads are 2N·m and 4N·m. The current chopping control strategy and the segmental PWM duty cycle analysis method based on current chopping control proposed in this paper are simulated respectively, and the current waveform and torque waveform under the two control strategies are compared.

In order to compare the torque ripple of the two control strategies, the torque ripple rate is defined.

$$K_m = \frac{T_{\max} - T_{\min}}{T_{av}} \times 100\% \tag{14}$$

In the formula, $T_{\max}$, $T_{\min}$, T_{av} are the maximum torque, the minimum torque and the given average torque, respectively.

Fig. 6 the speed is 500r/min and the load is 2N·m. Fig. 6(a) shows the current chopping control, and Fig. 6(b) shows the segmented PWM duty cycle analysis method. The current chopping control has a large current peak at the beginning of conduction, with a current peak of 7.8A, while the phase

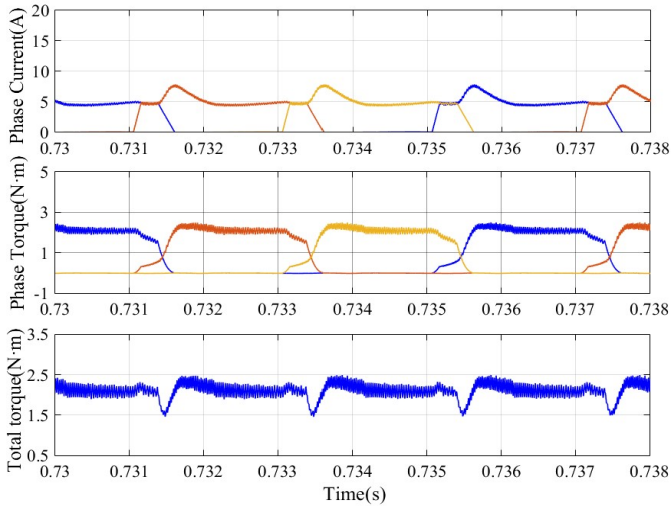

(a) Current chopper control

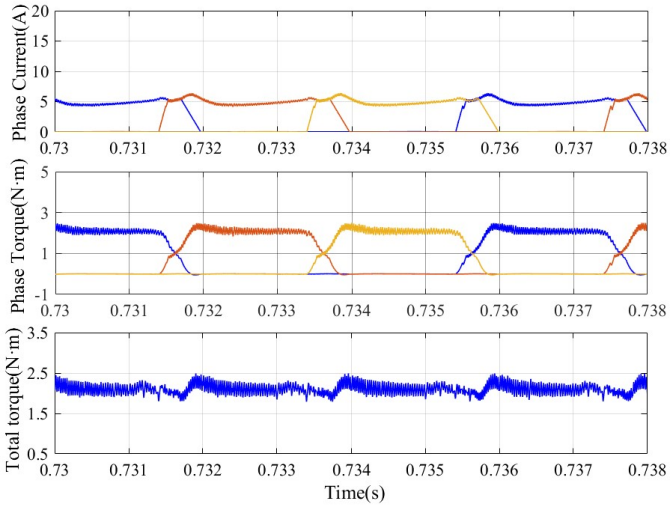

(b) Segment PWM duty cycle analysis method

Fig. 6. Waveform of three-phase current, three-phase torque and total torque (500r/min,2N).

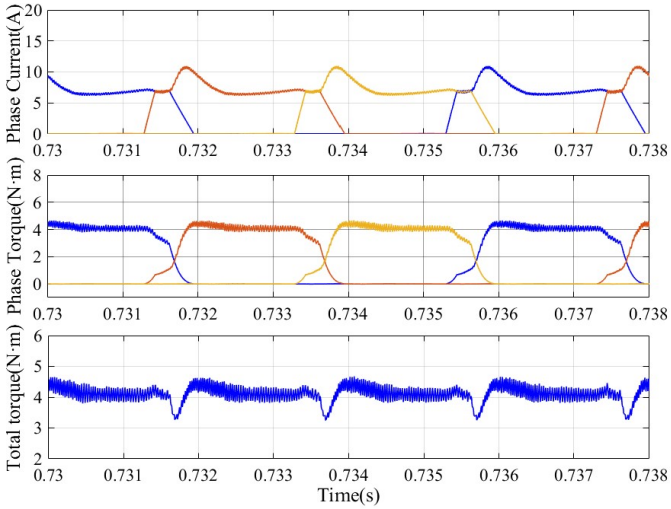

(a) Current chopper control

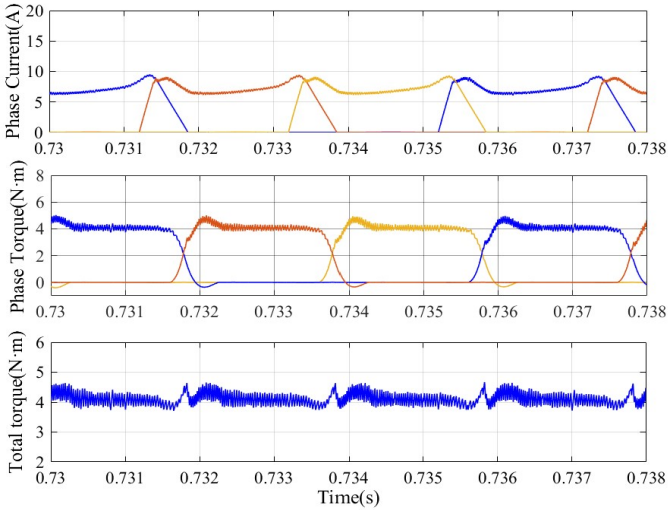

(b) Segment PWM duty cycle analysis method

Fig. 7. Waveform of three-phase current, three-phase torque and total torque (500r/min,4N).

current of the segmental PWM duty cycle analysis method is smoother, with a current peak of only 6.2A. And the torque ripple is also optimized. The torque of current chopping control

fluctuates in the interval (1.5,2.5), and the torque ripple reaches 50%. In contrast, the torque of the segmented PWM duty cycle analysis method fluctuates in the interval (1.73,2.5), and the torque ripple is reduced to 38.5%.

Fig. 7 the speed remains unchanged and the load is 4N·m. Fig. 7(a) shows the current chopping control, and Fig. 7(b) shows the segmented PWM duty cycle analysis method. As the load increases, the phase current increases accordingly, and the peak current of current chopping control current reaches 10.8A, while the peak current of phase current of segmented PWM duty cycle analysis method is 9.8A. The torque of current chopping control fluctuates in the interval (3.25,4.65), and the torque ripple is 35%. In contrast, the torque of the segmented PWM duty cycle analysis method fluctuates in the interval (3.82,4.65), and the torque ripple is only 20.75%.

Fig. 8 the speed is 750r/min and the load is 2N·m. Fig. 8(a) shows the current chopping control, and fig. 8(b) shows the segmented PWM duty cycle analysis method. The peak current of current chopping control is 7.4A. The phase current of the segmented PWM duty cycle analysis method is relatively stable, and the peak current is generally at the end of the small inductance region and the inductance rising region, with a peak value of 6.8A. In terms of torque ripple, the torque of the current chopping control fluctuates in the interval (1.5,2.5), and the torque ripple reaches 51%. The torque of the segmented PWM duty cycle analysis method fluctuates in the interval (1.73,2.52), and the torque ripple is reduced to 39.5%.

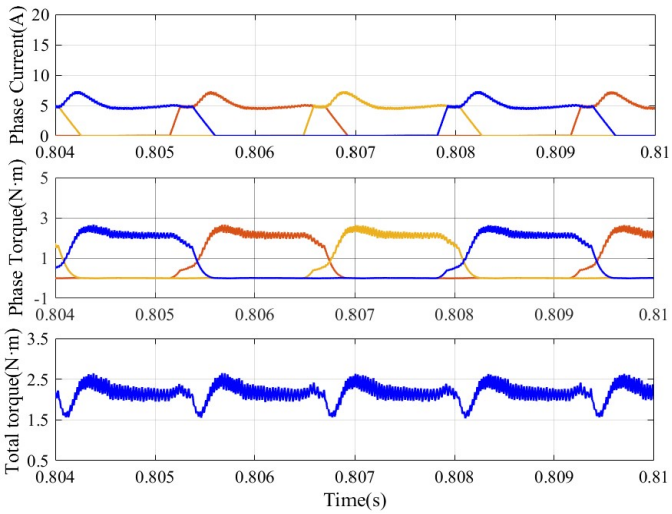

(a) Current chopper control

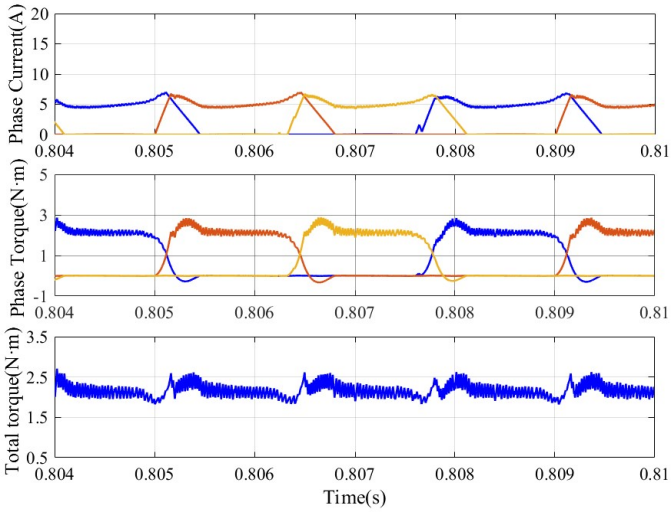

(b) Segment PWM duty cycle analysis method

Fig. 8. Waveform of three-phase current, three-phase torque and total torque (750r/min,2N).

Fig. 9 the load is 4N·m. Fig. 9(a) shows the current chopping control, and Fig. 9(b) shows the segmented PWM duty cycle analysis method. The peak current of current chopping control reaches 10.5A, while the peak current of phase current of segmented PWM duty cycle analysis method is 10A. The torque of the current chopping control fluctuates in the interval (3.3,4.7), and the torque ripple is 35%. The torque of the segmented PWM duty cycle analysis method fluctuates in the interval (3.85,4.6), and the torque ripple is only 18.75%.

From the above simulation results, it can be seen that the segmented PWM duty cycle analysis method has a great improvement in current peak and torque ripple suppression compared with the current chopping control. TABLE I shows the comparison of current peak and torque ripple between current chopping control and segmental PWM duty cycle analysis method.

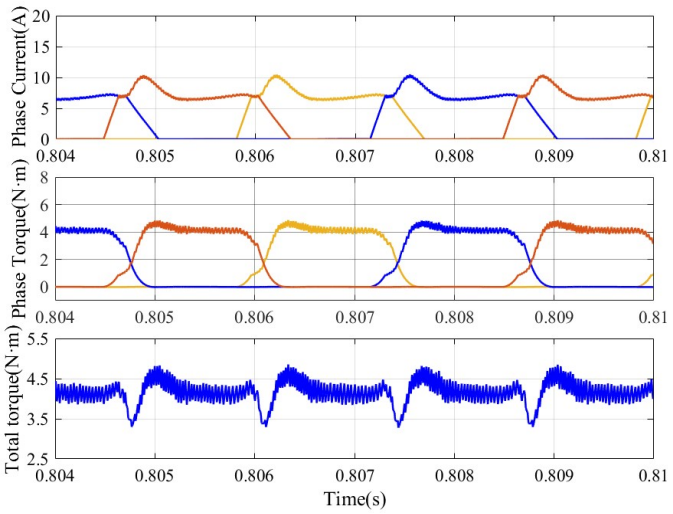

(a) Current chopper control

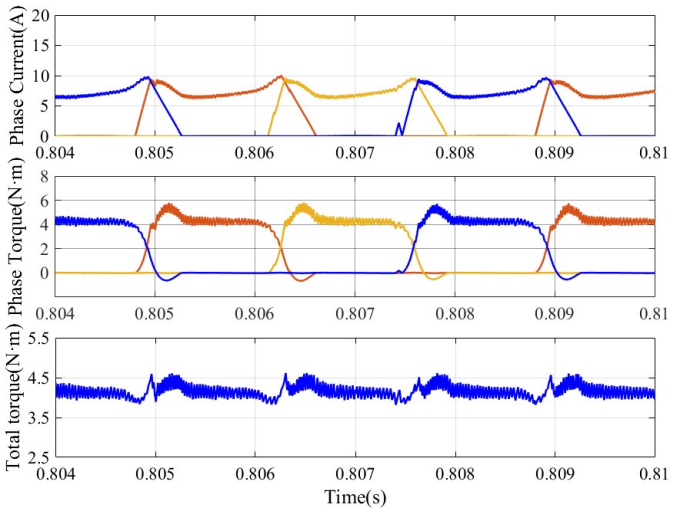

(b) Segment PWM duty cycle analysis method

Fig. 9. Waveform of three-phase current, three-phase torque and total torque (750r/min,4N).

TABLE I
COMPARISON OF CURRENT PEAK AND TORQUE RIPPLE SIMULATION RESULTS

control method	Motor speed(r/min)	load	current peak /A	torque ripple
current chopping control	500	2N	7.8	50%
		4N	10.8	35%
	750	2N	7.4	51%
		4N	10.5	35%
PWM duty cycle analysis method	500	2N	6.2	38.5%
		4N	9.8	20.75%
	750	2N	6.8	39.5%
		4N	10	18.75%

V. EXPERIMENTAL VERIFICATION

In order to further verify the effectiveness of the segmented PWM duty cycle analysis method proposed in this paper, an experimental platform of three-phase 6/20 SRM speed regulation system was built. The motor parameters of the experimental platform are consistent with those of the 6/20 SRM prototype in the simulation model. Fig. 10 shows the structure and assembly diagram of the experimental motor, and TABLE II shows the specific parameters of the experimental motor.

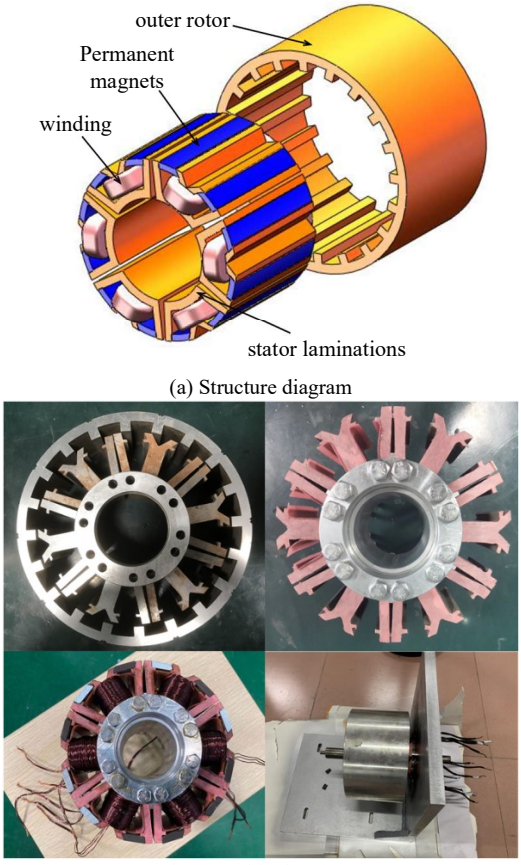

(a) Structure diagram

(b) assembly drawings

Fig. 10. Structure diagram and assembly drawing of SRM.

The motor experimental platform takes TMS320F28335DSP as the core controller, the drive board is a three-phase asymmetric half-bridge power converter, the rotor position angle of the motor is provided by a 15bit absolute encoder, and the load is provided by the magnetic powder brake, in addition to some sensors and measurement equipment. TABLE III shows the equipment list and important parameters of the motor experimental platform, and Fig. 11 shows the SRM experimental platform.

TABLE II
MOTOR PARAMETERS

Parameter	Value
Phase number	3
Stator and rotor poles	6/20
Rotor outer diameter (mm)	172
Rotor inner diameter (mm)	143.2
Stator outer diameter (mm)	142
Stator inner diameter (mm)	60
Stack length(mm)	100
length of air gap (mm)	0.6
Winding turns	55
Minimum inductance (mH)	5.8
Maximum inductance (mH)	13.6
Rated voltage (V)	540
Rated current (A)	30

TABLE III
THE EQUIPMENT LIST AND IMPORTANT PARAMETERS

Serial number	Equipment name	Model	main parameter
1	Torque sensor	HCNJ-101	0-100N·m
2	Magnetic powder brake	TZ100A-1	24V,0-100N·m
3	Oscilloscope	MSO4024	Four channels
4	Current probe	RP1001C	100A,300KHz
5	Current sensor	JCE50-ES	±50A,50KHz
6	Absolute encoder	BRT38COM32768	32768(15 bit)

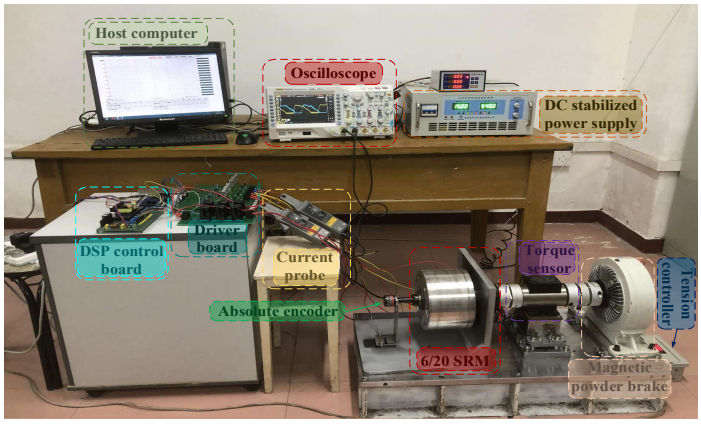

Fig. 11. SRM experimental platform.

Due to unavoidable factors, the waveforms obtained from the experiment are a little different from the simulation ideally, but on the whole it does not affect the verification of the experiment. In this paper, the data transfer rate of the torque sensor is 0.1 second, so the torque waveform is obtained by intercepting one minute of torque data in steady state.

The experimental results are shown in Fig. 12. In the experiment, the given load is 4N·m and the speed is 500 rpm. It can be seen from Fig. 12 that the phase current of the current chopping control has a large fluctuation in the chopping region with a peak value of 11 A, the torque fluctuates in the interval (2.8, 5.4) with a torque ripple of 65%. The phase current of the segmented PWM duty cycle analysis method is smoother in the chopping region with small fluctuations, with a peak value of only 10.3A, and the torque fluctuates in the interval (3.6,4.45), reducing the torque ripple to 21.25%.

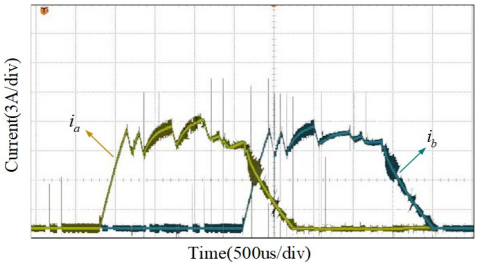

(a) Current waveform of Current chopper control

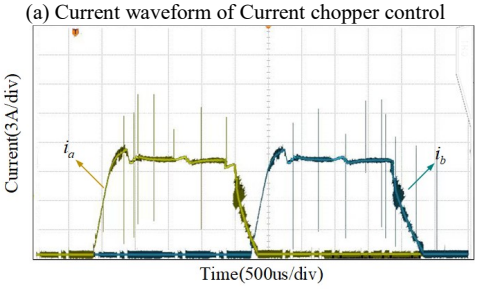

(b) Current waveform of Segment PWM duty cycle analysis method

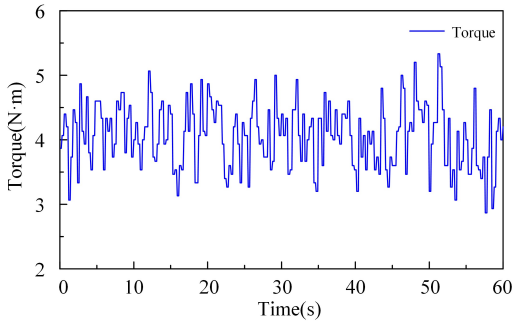

(c) Torque waveform of Current chopper control

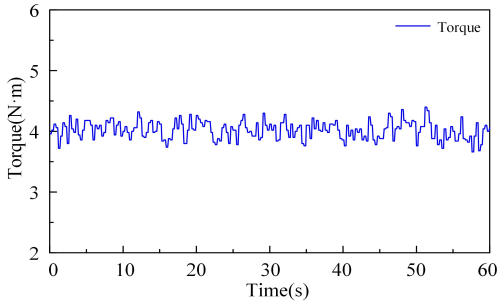

(d) Torque waveform of Segment PWM duty cycle analysis method

Fig. 12. Current and torque waveforms with a load of 4N·m at a speed of 500r/min.

The experimental results are shown in Fig. 13. In the experiment, the given load is 4N·m and the speed is 750 rpm. It can be seen from Fig. 13 that the phase current peak value of the current chopping control reaches 11.5A, the torque fluctuates in the interval (3.05,4.5), and the torque ripple is 36.25%. The phase current of the segmented PWM duty cycle analysis

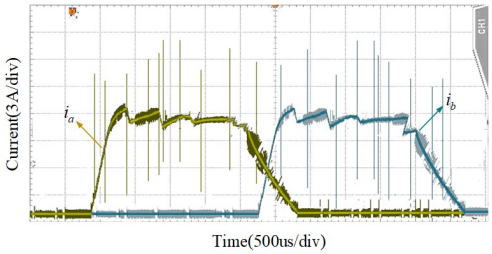

(a) Current waveform of Current chopper control

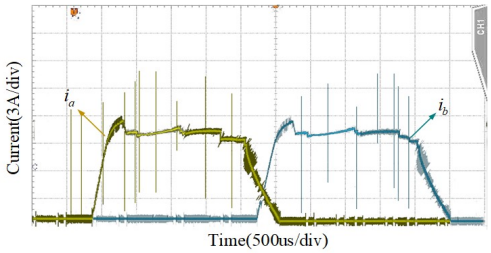

(b) Current waveform of Segment PWM duty cycle analysis method

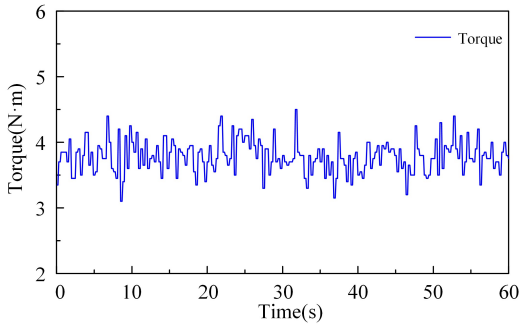

(c) Torque waveform of Current chopper control

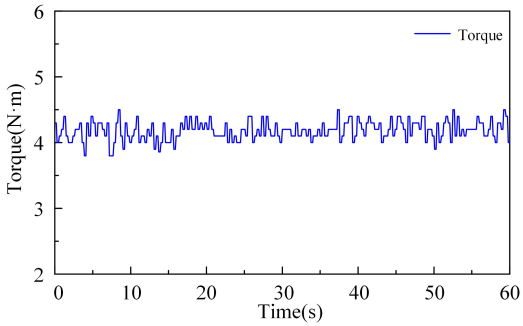

(d) Torque waveform of Segment PWM duty cycle analysis method

Fig. 13. Current and torque waveforms with a load of 4N·m at a speed of 750r/min.

method is less chopped in the chopping region, with a peak value is only 10.5A, and the torque fluctuates in the interval (3.75,4.5), and the torque ripple is reduced to 18.75%.

VI. Conclusion

In this paper, a segmented PWM duty cycle analysis method of Switched Reluctance Motor Based on current chopping control is proposed for the situation of large peak current and large torque ripple in actual control. According to the characteristic that the inductance value of the SRM winding in the small inductance region is approximately constant, the analytical formula for the PWM duty cycle in the small inductance region is derived. At the same time, the analytical formula for the PWM duty cycle in the inductor rise region is also derived based on the relationship between the inductance of the SRM winding in the inductor rise region and the rotor position angle as an approximate primary function. While current chopping control, the PWM duty cycle is used to adjust the average voltage at both ends of the conducting phase winding to realize the control of winding current. Finally, simulation experiments and motor platform experiments are carried out to verify the proposed method. The experimental results show that the control algorithm in this paper has less current peak and torque ripple compared with current chopping

control, and has high practical application value.

REFERENCES

[1] J. W. Ahn, G. F. Lukman, "Switched reluctance motor: Research trends and overview," *CES Transactions on Electrical Machines and Systems*, vol. 2, no. 4, pp. 339-347, 2018.

[2] X. C. Zhao, A. D. Xu and W. Zhang, "Research on DTC system with variable flux for switched reluctance motor," *CES Transactions on Electrical Machines and Systems*, vol. 1, no. 2, pp. 199-206, 2017.

[3] Q. N. Li, A. D. Xu and L. F. Zhou, "A Deadbeat Current Control Method for Switched Reluctance Motor," in *Proc. of Electromagnetics Research Letters*, vol. 91, pp. 123-128, 2020.

[4] X. Zhang, Q. Q. Yang, M. Y. Ma, et al., "A Switched Reluctance Motor Torque Ripple Reduction Strategy With Deadbeat Current Control and Active Thermal Management," *IEEE Transactions on Vehicular Technology*, vol. 69, no. 1, pp. 317-327, 2020.

[5] S. Q. Shen, H. Wang, Y. J. Feng, et al., "Predictive Current Control for Switched Reluctance Motor Based on Local Linear Phase Voltage Model," *Applied Sciences-Basel*, vol. 12, no. 3, 2020.

[6] S. K. Sahoo, S. K. Panda, J. X. Xu, et al., "Iterative learning-based high-performance current controller for switched reluctance motors," *IEEE Transactions on Energy Conversion*, vol. 19, no. 3, pp. 491-498, 2004.

[7] N. C. Sahoo, J. X. Xu and S. K. Panda, "Low torque ripple control of switched reluctance motors using iterative learning," *IEEE Transactions on Energy Conversion*, vol. 16, no. 4, pp. 318-326, 2002.

[8] H. Alharkan, S. Saadatmand, M. Ferdowsi, et al., "Optimal Tracking Current Control of Switched Reluctance Motor Drives Using Reinforcement Q-Learning Scheduling," *IEEE Access*, vol. 9, pp. 9926-9936, 2021.

[9] M. Y. Ma, F. Ling, Fei Li, et al., "Torque ripple suppression of switched reluctance motor by segmented harmonic currents injection based on adaptive fuzzy logic control," *IET Electric Power Applications*, vol. 14, no. 2, pp. 325-335, 2020.

[10] F. Peng, J. Ye and A. Emadi "A Digital PWM Current Controller for Switched Reluctance Motor Drives," *IEEE T rans. Power Electron*, vol. 31, pp. 7087–7098, 2015.

[11] H. Cai, H. Wang, M. Q. Li, et al., "Torque Ripple Reduction for Switched Reluctance Motor with Optimized PWM Control Strategy," *Energies*, vol. 11, no. 11, pp. 3215, 2018.

[12] N. Nakao, K. Akatsu, "Controlled Voltage Source Vector Control for Switched Reluctance Motors Using PWM Method," *Electrical Engineering in Japan*, vol. 198, no. 2, pp. 27-38, 2017.

[13] Y. Cheng, "Modified PWM Direct Instantaneous Torque Control System for SRM," *Mathematical Problems in Engineering*, 1-13, 2021.

[14] C. Zhao, J. J. Wang and H. Wang, "Simulation of direct instantaneous torque control and advanced direct instantaneous torque control for switched reluctance motor," *Journal of Mechanical & Electrical Engineering*, vol. 32, no. 5, pp. 626-631, 2015.

[15] H. Makino, T. Kosaka and N. Matsui, "Digital PWM-Control-Based Active Vibration Cancellation for Switched Reluctance Motors," *IEEE Transactions on Industry Applications*, vol. 51, no. 6, pp. 4521-4530, 2015.

[16] Z. Y. Yu, C. Gan, K. Ni, et al., "A Simplified PWM Strategy for Open-Winding Flux Modulated Doubly-Salient Reluctance Motor Drives with Switching Action Minimization," *IEEE Transactions on Industrial Electronics*, 1, 2022.

Chaozhi Huang was born in 1978 and received the B.S. degree in 2001. He received the M.S. degrees in detection technology and automation from Jiangxi University of Science and Technology, Ganzhou, China, in 2004. Later, he received the Ph.D degrees in Power System and Automation from Hohai University.

Since 1998, he has been with Jiangxi University of Science and Technology, where he is currently a professor in the School of Electrical Engineering and Automation. His research interests include motor structure design and drive control, robot control technology.

Yuliang Wu was born in Sichuan, China, in 1996. He received the B.S. degree in electrical engineering from Shanxi Agricultural University in 2019. He is currently working toward the M.S. degree in the electronic information from Jiangxi University of Science and Technology.

His current research interests include motor drive and control.

Hongwei Yuan was born in Xinzhou, China, in 1995. He received the B.S. degree in electrical engineering from Jiangxi University of Science and Technology in 2018. He is currently working toward the M.S. degree in the electrical engineering from Jiangxi University of Science and Technology.

His current research interests include switched reluctance motors and optimization algorithms.

Wensheng Cao was born in Shanxi, China, in1997. He received the B.S. degree in automation department from Taiyuan Industry College in 2020. He is currently working toward the M.S. degree in the electronic information from Jiangxi University of Science and Technology since 2020.

His research interests include the drive and control of switched reluctance motor.

Yongmin Geng was born in Henan, China, in 1997. He received the B.S. degree in electrical engineering from Henan Institute of Science and Technology in 2019. He is currently working toward the M.S. degree in electrical engineering from Jiangxi University of Science and Technology since 2020.

His research interests include optimal design of electrical machine structures.